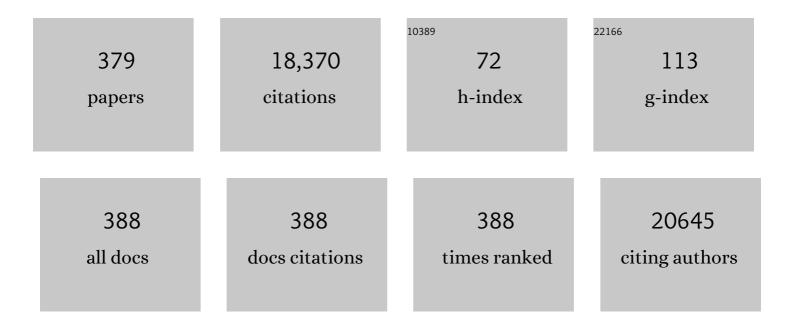
List of Publications by Year in descending order

Source: https://exaly.com/author-pdf/1667213/publications.pdf Version: 2024-02-01



FEDERICO ROSEL

#	Article	IF	CITATIONS
1	Bandgap tuning of multiferroic oxide solar cells. Nature Photonics, 2015, 9, 61-67.	31.4	640
2	Antibacterial Coatings: Challenges, Perspectives, and Opportunities. Trends in Biotechnology, 2015, 33, 637-652.	9.3	599
3	Properties of large organic molecules on metal surfaces. Progress in Surface Science, 2003, 71, 95-146.	8.3	419
4	Synthesis of Polyphenylene Molecular Wires by Surfaceâ€Confined Polymerization. Small, 2009, 5, 592-597.	10.0	314
5	Extending Polymer Conjugation into the Second Dimension. Science, 2009, 323, 216-217.	12.6	296
6	Supramolecular Assemblies on Surfaces: Nanopatterning, Functionality, and Reactivity. ACS Nano, 2018, 12, 7445-7481.	14.6	225
7	Nanostructured surfaces: challenges and frontiers in nanotechnology. Journal of Physics Condensed Matter, 2004, 16, S1373-S1436.	1.8	215
8	Gold nanoparticle decorated ceria nanotubes with significantly high catalytic activity for the reduction of nitrophenol and mechanism study. Applied Catalysis B: Environmental, 2013, 132-133, 107-115.	20.2	199
9	Tailoring the surface properties of Ti6Al4V by controlled chemical oxidation. Biomaterials, 2008, 29, 1285-1298.	11.4	197
10	Insight into Organometallic Intermediate and Its Evolution to Covalent Bonding in Surface-Confined Ullmann Polymerization. ACS Nano, 2013, 7, 8190-8198.	14.6	190
11	Synthesis of Ni–Ru Alloy Nanoparticles and Their High Catalytic Activity in Dehydrogenation of Ammonia Borane. Chemistry - A European Journal, 2012, 18, 7925-7930.	3.3	185
12	Molecular Selfâ€Assembly on Graphene. Small, 2014, 10, 1038-1049.	10.0	184
13	Near-IR Photoresponse in New Up-Converting CdSe/NaYF <sub>4</sub> :Yb,Er Nanoheterostructures. Journal of the American Chemical Society, 2010, 132, 8868-8869.	13.7	183
14	Improving Biocompatibility of Implantable Metals by Nanoscale Modification of Surfaces: An Overview of Strategies, Fabrication Methods, and Challenges. Small, 2009, 5, 996-1006.	10.0	182
15	Efficient and stable tandem luminescent solar concentrators based on carbon dots and perovskite quantum dots. Nano Energy, 2018, 50, 756-765.	16.0	170
16	Rational Modulation of the Periodicity in Linear Hydrogen-Bonded Assemblies of Trimesic Acid on Surfaces. Journal of the American Chemical Society, 2006, 128, 4212-4213.	13.7	169
17	Harnessing the properties of colloidal quantum dots in luminescent solar concentrators. Chemical Society Reviews, 2018, 47, 5866-5890.	38.1	169
18	Physical aspects of ferroelectric semiconductors for photovoltaic solar energy conversion. Physics Reports, 2016, 653, 1-40.	25.6	166

#	Article	IF	CITATIONS
19	Near Infrared, Highly Efficient Luminescent Solar Concentrators. Advanced Energy Materials, 2016, 6, 1501913.	19.5	161
20	Synthesis of mesoscale ordered two-dimensional π-conjugated polymers with semiconducting properties. Nature Materials, 2020, 19, 874-880.	27.5	158
21	Surface Nanopatterning to Control Cell Growth. Advanced Materials, 2008, 20, 1488-1492.	21.0	155
22	Perovskite quantum dots integrated in large-area luminescent solar concentrators. Nano Energy, 2017, 37, 214-223.	16.0	155
23	In situ facile synthesis of ruthenium nanocluster catalyst supported on carbon black for hydrogen generation from the hydrolysis of ammonia-borane. International Journal of Hydrogen Energy, 2012, 37, 17921-17927.	7.1	154
24	Remarkably enhanced photocatalytic activity of laser ablated Au nanoparticle decorated BiFeO3 nanowires under visible-light. Chemical Communications, 2013, 49, 5856.	4.1	154
25	Photovoltaic properties of Bi2FeCrO6 epitaxial thin films. Applied Physics Letters, 2011, 98, .	3.3	153
26	Colloidal carbon dots based highly stable luminescent solar concentrators. Nano Energy, 2018, 44, 378-387.	16.0	150
27	Two-Dimensional Structural Motif in Thienoacene Semiconductors: Synthesis, Structure, and Properties of Tetrathienoanthracene Isomers. Chemistry of Materials, 2008, 20, 2484-2494.	6.7	144
28	Maximizing Fieldâ€Effect Mobility and Solidâ€State Luminescence in Organic Semiconductors. Angewandte Chemie - International Edition, 2012, 51, 3837-3841.	13.8	135
29	Supramolecular Ordering in Oligothiopheneâ <sup>~,</sup> Fullerene Monolayers. Journal of the American Chemical Society, 2009, 131, 16844-16850.	13.7	134
30	Nanoscale Oxidative Patterning of Metallic Surfaces to Modulate Cell Activity and Fate. Nano Letters, 2009, 9, 659-665.	9.1	134
31	Crystal Engineering in Two Dimensions:  An Approach to Molecular Nanopatterning. Journal of Physical Chemistry C, 2007, 111, 16996-17007.	3.1	132
32	Synthesis and electronic structure of a two dimensional π-conjugated polythiophene. Chemical Science, 2013, 4, 3263.	7.4	130
33	Bifunctional catalytic/magnetic Ni@Ru core–shell nanoparticles. Chemical Communications, 2011, 47, 6308.	4.1	128
34	Heterocirculenes as a new class of organic semiconductors. Chemical Communications, 2008, , 5354.	4.1	126
35	Kinetics and thermodynamics in surface-confined molecular self-assembly. Chemical Science, 2011, 2, 2290.	7.4	122
36	Hybrid Carbon Nanotubes–TiO <sub>2</sub> Photoanodes for High Efficiency Dye-Sensitized Solar Cells. Journal of Physical Chemistry C, 2013, 117, 14510-14517.	3.1	121

#	Article	IF	CITATIONS
37	Halogen bonds in 2D supramolecular self-assembly of organic semiconductors. Nanoscale, 2012, 4, 5965.	5.6	120
38	Step-by-step growth of epitaxially aligned polythiophene by surface-confined reaction. Proceedings of the United States of America, 2010, 107, 11200-11204.	7.1	117
39	Heavy metal-free, near-infrared colloidal quantum dots for efficient photoelectrochemical hydrogen generation. Nano Energy, 2017, 31, 441-449.	16.0	116
40	SCANNING TUNNELING MICROSCOPY MANIPULATION OF COMPLEX ORGANIC MOLECULES ON SOLID SURFACES. Annual Review of Physical Chemistry, 2006, 57, 497-525.	10.8	114
41	Absorption Enhancement in "Giant―Core/Alloyed-Shell Quantum Dots for Luminescent Solar Concentrator. Small, 2016, 12, 5354-5365.	10.0	112
42	Interfacial Reactionâ€Directed Synthesis of Ce–Mn Binary Oxide Nanotubes and Their Applications in CO Oxidation and Water Treatment. Advanced Functional Materials, 2012, 22, 3914-3920.	14.9	110
43	Solvent-Antisolvent Ambient Processed Large Grain Size Perovskite Thin Films for High-Performance Solar Cells. Scientific Reports, 2018, 8, 12885.	3.3	109
44	Colloidal Quantum Dots for Solar Technologies. CheM, 2017, 3, 229-258.	11.7	107
45	Ullmann-type coupling of brominated tetrathienoanthracene on copper and silver. Nanoscale, 2014, 6, 2660-2668.	5.6	106
46	Multiple NaNbO <sub>3</sub> /Nb <sub>2</sub> O <sub>5</sub> Heterostructure Nanotubes: A New Class of Ferroelectric/Semiconductor Nanomaterials. Advanced Materials, 2010, 22, 1741-1745.	21.0	104
47	High efficiency, Pt-free photoelectrochemical cells for solar hydrogen generation based on "giant― quantum dots. Nano Energy, 2016, 27, 265-274.	16.0	103
48	Two-Dimensional Nanotemplates as Surface Cues for the Controlled Assembly of Organic Molecules. Topics in Current Chemistry, 2008, 285, 203-267.	4.0	102
49	Supramolecular assembly of heterocirculenes in 2D and 3D. Chemical Communications, 2009, , 1192.	4.1	100
50	One-Dimensional Assembly and Selective Orientation of Lander Molecules on an O–Cu Template. Angewandte Chemie - International Edition, 2004, 43, 2092-2095.	13.8	99
51	Characterization of a bioactive nanotextured surface created by controlled chemical oxidation of titanium. Surface Science, 2006, 600, 4613-4621.	1.9	98
52	Core/Shell Quantum Dots Solar Cells. Advanced Functional Materials, 2020, 30, 1908762.	14.9	98
53	Highly Stable Colloidal "Giant―Quantum Dots Sensitized Solar Cells. Advanced Functional Materials, 2017, 27, 1701468.	14.9	92
54	Halogen bonds as stabilizing interactions in a chiral self-assembled molecular monolayer. Chemical Communications, 2011, 47, 9453.	4.1	91

#	Article	IF	CITATIONS
55	Lanthanide Ion Doped Upconverting Nanoparticles: Synthesis, Structure and Properties. Small, 2016, 12, 3888-3907.	10.0	91
56	Quasi one-dimensional band dispersion and surface metallization in long-range ordered polymeric wires. Nature Communications, 2016, 7, 10235.	12.8	91
57	Stabilization of exotic minority phases in a multicomponent self-assembled molecular network. Nanotechnology, 2007, 18, 424031.	2.6	90
58	Nearâ€Infrared, Heavy Metalâ€Free Colloidal "Giant―Core/Shell Quantum Dots. Advanced Energy Materials, 2018, 8, 1701432.	19.5	90
59	Engineering interfacial structure in "Giant―PbS/CdS quantum dots for photoelectrochemical solar energy conversion. Nano Energy, 2016, 30, 531-541.	16.0	88
60	A solution to break the salt barrier for high-rate sustainable solar desalination. Energy and Environmental Science, 2021, 14, 2451-2459.	30.8	87
61	Ternary organic solar cells: A review of the role of the third element. Nano Energy, 2022, 94, 106915.	16.0	87
62	Mega High Utilization of Sodium Metal Anodes Enabled by Single Zinc Atom Sites. Nano Letters, 2019, 19, 7827-7835.	9.1	86
63	Improved photovoltaic performance from inorganic perovskite oxide thin films with mixed crystal phases. Nature Photonics, 2018, 12, 271-276.	31.4	84
64	Hole-extraction and photostability enhancement in highly efficient inverted perovskite solar cells through carbon dot-based hybrid material. Nano Energy, 2019, 62, 781-790.	16.0	83
65	Controlling photoinduced electron transfer from PbS@CdS core@shell quantum dots to metal oxide nanostructured thin films. Nanoscale, 2014, 6, 7004-7011.	5.6	81
66	Mechanistic Picture and Kinetic Analysis of Surface-Confined Ullmann Polymerization. Journal of the American Chemical Society, 2016, 138, 16696-16702.	13.7	81
67	Enhanced photovoltaic properties in dye sensitized solar cells by surface treatment of SnO2 photoanodes. Scientific Reports, 2016, 6, 23312.	3.3	80
68	Efficient Upconverting Multiferroic Core@Shell Photocatalysts: Visible-to-Near-Infrared Photon Harvesting. ACS Applied Materials & Interfaces, 2017, 9, 8142-8150.	8.0	79
69	Facile Synthesis of Nanosheet-like CuO Film and its Potential Application as a High-Performance Pseudocapacitor Electrode. Electrochimica Acta, 2016, 198, 220-230.	5.2	77
70	Reduced graphene oxide growth on 316L stainless steel for medical applications. Nanoscale, 2014, 6, 8664-8670.	5.6	76
71	Nearâ€Infrared Colloidal Quantum Dots for Efficient and Durable Photoelectrochemical Solarâ€Đriven Hydrogen Production. Advanced Science, 2016, 3, 1500345.	11.2	76
72	Covalently bonded networks through surface-confined polymerization. Surface Science, 2013, 613, 6-14.	1.9	75

#	Article	IF	CITATIONS
73	Diatom frustules as light traps enhance DSSC efficiency. Nanoscale, 2013, 5, 873-876.	5.6	74
74	Epitaxial Bi <sub>2</sub> FeCrO <sub>6</sub> Multiferroic Thin Film as a New Visible Light Absorbing Photocathode Material. Small, 2015, 11, 4018-4026.	10.0	73
75	Surface-confined single-layer covalent organic frameworks: design, synthesis and application. Chemical Society Reviews, 2020, 49, 2020-2038.	38.1	73
76	Encapsulated cobalt nanoparticles as a recoverable catalyst for the hydrolysis of sodium borohydride. Energy Storage Materials, 2020, 27, 187-197.	18.0	72
77	Platinum Cluster/Carbon Quantum Dots Derived Graphene Heterostructured Carbon Nanofibers for Efficient and Durable Solarâ€Driven Electrochemical Hydrogen Evolution. Small Methods, 2022, 6, e2101470.	8.6	72
78	Graphene below the percolation threshold in TiO <sub>2</sub> for dye-sensitized solar cells. Journal of Materials Chemistry A, 2015, 3, 2580-2588.	10.3	70
79	Functionalized multi-wall carbon nanotubes/TiO <sub>2</sub> composites as efficient photoanodes for dye sensitized solar cells. Journal of Materials Chemistry C, 2016, 4, 3555-3562.	5.5	68
80	Approaches for ultrafast imaging of transient materials processes in the transmission electron microscope. Micron, 2012, 43, 1108-1120.	2.2	67
81	Manipulation of charge transfer in vertically aligned epitaxial ferroelectric KNbO3 nanowire array photoelectrodes. Nano Energy, 2017, 35, 92-100.	16.0	67
82	Epitaxial Patterning of Bi <sub>2</sub> FeCrO <sub>6</sub> Double Perovskite Nanostructures: Multiferroic at Room Temperature. Advanced Materials, 2011, 23, 1724-1729.	21.0	66
83	Hollow ruthenium nanoparticles with small dimensions derived from Ni@Ru core@shell structure: synthesis and enhanced catalytic dehydrogenation of ammonia borane. Chemical Communications, 2012, 48, 8009.	4.1	66
84	Effect of multi-walled carbon nanotubes on the stability of dye sensitized solar cells. Journal of Power Sources, 2013, 233, 93-97.	7.8	66
85	Substrate Effects in the Supramolecular Assembly of 1,3,5-Benzene Tricarboxylic Acid on Graphite and Graphene. Langmuir, 2015, 31, 7016-7024.	3.5	63
86	Optoelectronic Properties in Nearâ€Infrared Colloidal Heterostructured Pyramidal "Giant―Core/Shell Quantum Dots. Advanced Science, 2018, 5, 1800656.	11.2	63
87	Phase-junction design of MOF-derived TiO2 photoanodes sensitized with quantum dots for efficient hydrogen generation. Applied Catalysis B: Environmental, 2020, 263, 118317.	20.2	63
88	Upconverting nanocomposites with combined photothermal and photodynamic effects. Nanoscale, 2018, 10, 791-799.	5.6	61
89	Complex oxide nanostructures by pulsed laser deposition through nanostencils. Applied Physics Letters, 2005, 86, 183107.	3.3	60
90	Rough Fibrils Provide a Toughening Mechanism in Biological Fibers. ACS Nano, 2012, 6, 1961-1969.	14.6	59

#	Article	IF	CITATIONS
91	Evidence of antibacterial activity on titanium surfaces through nanotextures. Applied Surface Science, 2014, 308, 275-284.	6.1	59
92	Substrate, Molecular Structure, and Solvent Effects in 2D Self-Assembly via Hydrogen and Halogen Bonding. Journal of Physical Chemistry C, 2014, 118, 25505-25516.	3.1	59
93	Multifunctional Liposome Nanocarriers Combining Upconverting Nanoparticles and Anticancer Drugs. Journal of Physical Chemistry B, 2016, 120, 4992-5001.	2.6	58
94	A single multifunctional nanoplatform based on upconversion luminescence and gold nanorods. Nanoscale, 2015, 7, 5178-5185.	5.6	57
95	Ultrafast and high-efficient self-healing epoxy coatings with active multiple hydrogen bonds for corrosion protection. Corrosion Science, 2021, 187, 109485.	6.6	56
96	Unprecedented Transformation of Tetrathienoanthracene into Pentacene on Ni(111). ACS Nano, 2013, 7, 1652-1657.	14.6	54
97	Size Dependence of Temperature-Related Optical Properties of PbS and PbS/CdS Core/Shell Quantum Dots. Journal of Physical Chemistry C, 2014, 118, 20585-20593.	3.1	54
98	Long-term stability of hydrogenated DLC coatings: Effects of aging on the structural, chemical and mechanical properties. Diamond and Related Materials, 2014, 48, 65-72.	3.9	54
99	Dual emission in asymmetric "giant―PbS/CdS/CdS core/shell/shell quantum dots. Nanoscale, 2016, 8, 4217-4226.	5.6	54
100	The role of halogens in on-surface Ullmann polymerization. Faraday Discussions, 2017, 204, 453-469.	3.2	54
101	Multiferroic Bi <sub>2</sub> FeCrO <sub>6</sub> based p–i–n heterojunction photovoltaic devices. Journal of Materials Chemistry A, 2017, 5, 10355-10364.	10.3	53
102	Lithium dendrite inhibition via 3D porous lithium metal anode accompanied by inherent SEI layer. Energy Storage Materials, 2020, 26, 385-390.	18.0	52
103	Structure/Property Relations in "Giant―Semiconductor Nanocrystals: Opportunities in Photonics and Electronics. Accounts of Chemical Research, 2018, 51, 609-618.	15.6	51
104	Single-cluster Au as an usher for deeply cyclable Li metal anodes. Journal of Materials Chemistry A, 2019, 7, 14496-14503.	10.3	51
105	Quantum Dotsâ€Based Photoelectrochemical Hydrogen Evolution from Water Splitting. Advanced Energy Materials, 2021, 11, 2003233.	19.5	51
106	Photoluminescent silicon nanocrystals synthesized by reactive laser ablation. Applied Physics Letters, 2006, 88, 073105.	3.3	49
107	Environmentally stable light emitting field effect transistors based on 2-(4-pentylstyryl)tetracene. Journal of Materials Chemistry, 2008, 18, 158-161.	6.7	49
108	Adsorption of proteins on nanoporous Ti surfaces. Surface Science, 2010, 604, 1445-1451.	1.9	49

#	Article	IF	CITATIONS
109	Sustainable sensors from silk. Nature Materials, 2013, 12, 98-100.	27.5	49
110	Ultrafast Microwave Hydrothermal Synthesis of <scp><scp>BiFeO</scp></scp> <sub>3</sub> Nanoplates. Journal of the American Ceramic Society, 2013, 96, 3155-3162.	3.8	49
111	1,5-, 2,6- and 9,10-distyrylanthracenes as luminescent organic semiconductors. Journal of Materials Chemistry C, 2013, 1, 2817.	5.5	48
112	Solution and air stable host/guest architectures from a single layer covalent organic framework. Chemical Communications, 2015, 51, 16510-16513.	4.1	48
113	Ultrasmall PbS quantum dots: a facile and greener synthetic route and their high performance in luminescent solar concentrators. Journal of Materials Chemistry A, 2017, 5, 10250-10260.	10.3	48
114	Photovoltaic effect in multiphase Bi-Mn-O thin films. Optics Express, 2014, 22, A80.	3.4	46
115	Electrospun ceramic nanofibers as 1D solid electrolytes for lithium batteries. Electrochemistry Communications, 2019, 104, 106483.	4.7	46
116	Efficient solar-driven hydrogen generation using colloidal heterostructured quantum dots. Journal of Materials Chemistry A, 2019, 7, 14079-14088.	10.3	46
117	lodine-assisted antisolvent engineering for stable perovskite solar cells with efficiency >21.3 %. Nano Energy, 2020, 67, 104224.	16.0	46
118	"Greenâ€; gradient multi-shell CuInSe2/(CuInSexS1-x)5/CuInS2 quantum dots for photo-electrochemical hydrogen generation. Applied Catalysis B: Environmental, 2021, 280, 119402.	20.2	46
119	Nucleation and growth of Si nanocrystals in an amorphousSiO2matrix. Physical Review B, 2006, 74, .	3.2	45
120	The elastic moduli of oriented tin oxide nanowires. Nanotechnology, 2009, 20, 115705.	2.6	44
121	Enhanced conversion efficiency in Si solar cells employing photoluminescent down-shifting CdSe/CdS core/shell quantum dots. Scientific Reports, 2017, 7, 14104.	3.3	44
122	Heterostructured quantum dot architectures for efficient and stable photoelectrochemical hydrogen production. Journal of Materials Chemistry A, 2018, 6, 6822-6829.	10.3	44
123	Iron (II) phthalocyanine/N-doped graphene: A highly efficient non-precious metal catalyst for oxygen reduction. International Journal of Hydrogen Energy, 2019, 44, 18103-18114.	7.1	44
124	Interfacial engineering in colloidal "giant―quantum dots for high-performance photovoltaics. Nano Energy, 2019, 55, 377-388.	16.0	44
125	Asymmetric Silver "Nanocarrot―Structures: Solution Synthesis and Their Asymmetric Plasmonic Resonances. Journal of the American Chemical Society, 2013, 135, 9616-9619.	13.7	43
126	Fluidic patch antenna based on liquid metal alloy/single-wall carbon-nanotubes operating at the S-band frequency. Applied Physics Letters, 2013, 103, .	3.3	43

#	Article	IF	CITATIONS
127	Ultrasensitive, Biocompatible, Selfâ€Calibrating, Multiparametric Temperature Sensors. Small, 2015, 11, 5741-5746.	10.0	43
128	Nanoporous twinned PtPd with highly catalytic activity and stability. Journal of Materials Chemistry A, 2015, 3, 2050-2056.	10.3	43
129	Plasmonic Glasses and Films Based on Alternative Inexpensive Materials for Blocking Infrared Radiation. Nano Letters, 2018, 18, 3147-3156.	9.1	43
130	First-principles study on ZnV2O6 and Zn2V2O7: Two new photoanode candidates for photoelectrochemical water oxidation. Ceramics International, 2018, 44, 6607-6613.	4.8	43
131	Efficient and stable photoelectrochemical hydrogen generation using optimized colloidal heterostructured quantum dots. Nano Energy, 2021, 79, 105416.	16.0	43
132	Atomic description of elementary surface processes: diffusion and dynamics. Surface Science, 2002, 500, 395-413.	1.9	42
133	Synthesis of graphene–ZnO nanocomposites by a one-step electrochemical deposition for efficient photocatalytic degradation of organic pollutant. Solid State Sciences, 2019, 98, 106039.	3.2	42
134	Hierarchically Porous Cu-, Co-, and Mn-Doped Platelet-Like ZnO Nanostructures and Their Photocatalytic Performance for Indoor Air Quality Control. ACS Omega, 2019, 4, 16429-16440.	3.5	42
135	Unravelling the Self-Assembly of Hydrogen Bonded NDI Semiconductors in 2D and 3D. Chemistry of Materials, 2016, 28, 951-961.	6.7	41
136	Long-range ordered and atomic-scale control of graphene hybridization by photocycloaddition. Nature Chemistry, 2020, 12, 1035-1041.	13.6	41
137	Tunable hierarchical surfaces of CuO derived from metal–organic frameworks for non-enzymatic glucose sensing. Inorganic Chemistry Frontiers, 2020, 7, 1512-1525.	6.0	41
138	Nanocrystallization of amorphous germanium films observed with nanosecond temporal resolution. Applied Physics Letters, 2010, 97, .	3.3	40
139	Enhanced photovoltaic properties in bilayer BiFeO3/Bi-Mn-O thin films. Nanotechnology, 2016, 27, 215402.	2.6	40
140	Epitaxial Bi <sub>2</sub> FeCrO <sub>6</sub> Multiferroic Thin-Film Photoanodes with Ultrathin p-Type NiO Layers for Improved Solar Water Oxidation. ACS Applied Materials & Interfaces, 2019, 11, 13185-13193.	8.0	40
141	Photocatalytic Activity of ZnV <sub>2</sub> O <sub>6</sub> /Reduced Graphene Oxide Nanocomposite: From Theory to Experiment. Journal of the Electrochemical Society, 2018, 165, H353-H359.	2.9	39
142	Controlled synthesis of graphene via electrochemical route and its use as efficient metal-free catalyst for oxygen reduction. Applied Catalysis B: Environmental, 2019, 243, 373-380.	20.2	39
143	Synergistic Effect of Plasmonic Gold Nanoparticles Decorated Carbon Nanotubes in Quantum Dots/TiO <sub>2</sub> for Optoelectronic Devices. Advanced Science, 2020, 7, 2001864.	11.2	39
144	A novel approach to the synthesis of photoluminescent germanium nanoparticles by reactive laser ablation. Nanotechnology, 2006, 17, 2152-2155.	2.6	38

#	Article	IF	CITATIONS
145	Shape-controlled synthesis of ruthenium nanocrystals and their catalytic applications. New Journal of Chemistry, 2014, 38, 1827-1833.	2.8	38
146	Hybrid TiO2-Graphene nanoribbon photoanodes to improve the photoconversion efficiency of dye sensitized solar cells. Journal of Power Sources, 2018, 396, 566-573.	7.8	38
147	Highly stable photoelectrochemical cells for hydrogen production using a SnO <sub>2</sub> –TiO <sub>2</sub> /quantum dot heterostructured photoanode. Nanoscale, 2018, 10, 15273-15284.	5.6	38
148	Two-Dimensional Self-Assembly of a Symmetry-Reduced Tricarboxylic Acid. Langmuir, 2013, 29, 7318-7324.	3.5	37
149	Ordered Assembly of α-Quinquethiophene on a Copper Oxide Nanotemplate. Small, 2006, 2, 1366-1371.	10.0	36
150	Photovoltaic Properties of Multiferroic BiFeO <sub>3</sub> /BiCrO <sub>3</sub> Heterostructures. Journal of the American Ceramic Society, 2014, 97, 1837-1840.	3.8	36
151	Platinum/Palladium hollow nanofibers as high-efficiency counter electrodes for enhanced charge transfer. Journal of Power Sources, 2016, 335, 138-145.	7.8	36
152	Highly efficient and stable spray assisted nanostructured Cu2S/Carbon paper counter electrode for quantum dots sensitized solar cells. Journal of Power Sources, 2019, 436, 226849.	7.8	36
153	Insight into phosphate doped BiVO4 heterostructure for multifunctional photocatalytic performances: A combined experimental and DFT study. Applied Surface Science, 2019, 466, 787-800.	6.1	36
154	Review of Hybrid 1D/2D Photocatalysts for Light-Harvesting Applications. ACS Applied Nano Materials, 2021, 4, 11323-11352.	5.0	36
155	Influence of Treatment Conditions on the Chemical Oxidative Activity of H <sub>2</sub> SO <sub>4</sub> /H <sub>2</sub> O <sub>2</sub> Mixtures for Modulating the Topography of Titanium. Advanced Engineering Materials, 2009, 11, B227.	3.5	35
156	The critical role of water in spider silk and its consequence for protein mechanics. Nanoscale, 2011, 3, 3805.	5.6	35
157	Nanoporous copper-cobalt mixed oxide nanorod bundles as high performance pseudocapacitive electrodes. Journal of Electroanalytical Chemistry, 2017, 787, 24-35.	3.8	35
158	Control of Fullerene Crystallization from 2D to 3D through Combined Solvent and Template Effects. Journal of the American Chemical Society, 2017, 139, 16732-16740.	13.7	35
159	A 2D Substitutional Solid Solution through Hydrogen Bonding of Molecular Building Blocks. ACS Nano, 2017, 11, 8901-8909.	14.6	35
160	Visible and Near-Infrared, Multiparametric, Ultrasensitive Nanothermometer Based on Dual-Emission Colloidal Quantum Dots. ACS Photonics, 2019, 6, 2479-2486.	6.6	35
161	Recent progress in nanostructured multiferroic Bi2FeCrO6 thin films. Journal of Solid State Chemistry, 2012, 189, 13-20.	2.9	34
162	In Situ Formation of Dendrites in Eumelanin Thin Films between Gold Electrodes. Advanced Functional Materials, 2013, 23, 5591-5598.	14.9	34

#	Article	IF	CITATIONS
163	Complex crystallization dynamics in amorphous germanium observed with dynamic transmission electron microscopy. Physical Review B, 2013, 87, .	3.2	34
164	Interfacial reaction-directed synthesis of a ceria nanotube-embedded ultra-small Pt nanoparticle catalyst with high catalytic activity and thermal stability. Journal of Materials Chemistry A, 2016, 4, 14148-14154.	10.3	34
165	Combined magnetron sputtering and pulsed laser deposition of TiO 2 and BFCO thin films. Scientific Reports, 2017, 7, 2503.	3.3	34
166	3D low toxicity Cu–Pb binary perovskite films and their photoluminescent/photovoltaic performance. Journal of Materials Chemistry A, 2019, 7, 27225-27235.	10.3	34
167	Eco-friendly quantum dots for liquid luminescent solar concentrators. Journal of Materials Chemistry A, 2020, 8, 1787-1798.	10.3	34
168	Evolution of the intermixing process in Ge/Si(111) self-assembled islands. Materials Science and Engineering B: Solid-State Materials for Advanced Technology, 2002, 88, 264-268.	3.5	33
169	Template engaged synthesis of hollow ceria-based composites. Nanoscale, 2015, 7, 5578-5591.	5.6	33
170	A colloidal heterostructured quantum dot sensitized carbon nanotube–TiO <sub>2</sub> hybrid photoanode for high efficiency hydrogen generation. Nanoscale Horizons, 2019, 4, 404-414.	8.0	33
171	Highly Compact TiO <sub>2</sub> Films by Spray Pyrolysis and Application in Perovskite Solar Cells. Advanced Engineering Materials, 2019, 21, 1801196.	3.5	33
172	Environmentally friendly Mn-alloyed core/shell quantum dots for high-efficiency photoelectrochemical cells. Journal of Materials Chemistry A, 2020, 8, 10736-10741.	10.3	33
173	Selective Adsorption of Pyridine at Isolated Reactive Sites on Si(100). Journal of Physical Chemistry B, 2005, 109, 20055-20059.	2.6	32
174	Effects of Fe concentration on properties of ZnO nanostructures and their application to photocurrent generation. Solid State Sciences, 2019, 92, 76-80.	3.2	32
175	Hybrid graphene/metal oxide anodes for efficient and stable dye sensitized solar cell. Electrochimica Acta, 2020, 349, 136409.	5.2	32
176	Mesenchymal Stem Cell-Laden Hydrogel Microfibers for Promoting Nerve Fiber Regeneration in Long-Distance Spinal Cord Transection Injury. ACS Biomaterials Science and Engineering, 2020, 6, 1165-1175.	5.2	32
177	Self-assembly of Rubrene on Copper Surfaces. Journal of Physical Chemistry C, 2008, 112, 10214-10221.	3.1	31
178	Single-crystalline BiFeO3 nanowires and their ferroelectric behavior. Applied Physics Letters, 2012, 101, 192903.	3.3	31
179	Photovoltaic properties of Bi <sub>2</sub> FeCrO <sub>6</sub> films epitaxially grown on (100)-oriented silicon substrates. Nanoscale, 2016, 8, 3237-3243.	5.6	31
180	Highly Sensitive Switchable Heterojunction Photodiode Based on Epitaxial Bi <sub>2</sub> FeCrO <sub>6</sub> Multiferroic Thin Films. ACS Applied Materials & Interfaces, 2018, 10, 12790-12797.	8.0	31

#	Article	IF	CITATIONS
181	Morphology Control of Lanthanide Doped NaGdF <sub>4</sub> Nanocrystals via One-Step Thermolysis. Chemistry of Materials, 2019, 31, 5160-5171.	6.7	31
182	Structure/Property Control in Photocatalytic Organic Semiconductor Nanocrystals. Advanced Functional Materials, 2021, 31, 2104099.	14.9	31
183	Enormous Surfaceâ€Enhanced Raman Scattering from Dimers of Flowerâ€Like Silver Mesoparticles. Small, 2012, 8, 3400-3405.	10.0	30
184	Pulsed laser deposition growth of rutile TiO2 nanowires on Silicon substrates. Applied Surface Science, 2014, 313, 48-52.	6.1	30
185	Dynamics of semiconducting nanocrystal uptake into mesoporous TiO <sub>2</sub> thick films by electrophoretic deposition. Journal of Materials Chemistry A, 2015, 3, 847-856.	10.3	30
186	Ultrasmall Nanoplatelets: The Ultimate Tuning of Optoelectronic Properties. Advanced Energy Materials, 2017, 7, 1602728.	19.5	30
187	Self-assembled monolayer of alkanephosphoric acid on nanotextured Ti. Journal of Chemical Physics, 2008, 128, 144705.	3.0	29
188	An unexpected organometallic intermediate in surface-confined Ullmann coupling. Nanoscale, 2019, 11, 7682-7689.	5.6	29
189	Chemical Mapping of Individual Semiconductor Nanostructures. Small, 2006, 2, 401-405.	10.0	28
190	Order and disorder in the heteroepitaxy of semiconductor nanostructures. Materials Science and Engineering Reports, 2010, 70, 243-264.	31.8	28
191	Spider silk as a load bearing biomaterial: tailoring mechanical properties via structural modifications. Nanoscale, 2011, 3, 870.	5.6	28
192	Organic analogues of graphene. Nature, 2017, 542, 423-424.	27.8	28
193	Surface-mediated assembly, polymerization and degradation of thiophene-based monomers. Chemical Science, 2019, 10, 5167-5175.	7.4	28
194	Nanoelectromagnetic of a highly conductive 2D transition metal carbide (MXene)/Graphene nanoplatelets composite in the EHF M-band frequency. Carbon, 2021, 173, 528-539.	10.3	28
195	Epitaxial magnetite nanorods with enhanced room temperature magnetic anisotropy. Nanoscale, 2017, 9, 7858-7867.	5.6	27
196	Selective binding in different adsorption sites of a 2D covalent organic framework. CrystEngComm, 2017, 19, 4927-4932.	2.6	27
197	Probing functional self-assembled molecular architectures with solution/solid scanning tunnelling microscopy. Chemical Communications, 2018, 54, 10527-10539.	4.1	27
198	Correlation between plasma dynamics and porosity of Ge films synthesized by pulsed laser deposition. Applied Physics Letters, 2006, 89, 131501.	3.3	26

#	Article	IF	CITATIONS
199	Electromagnetic energy absorption potential and microwave heating capacity of SiC thin films in the 1–16GHz frequency range. Applied Surface Science, 2012, 258, 5482-5485.	6.1	26
200	Effect of Redox Reaction Products on the Luminescence Switching Behavior in CePO <sub>4</sub> :Tb Nanorods. Journal of Physical Chemistry C, 2013, 117, 10031-10038.	3.1	26
201	Development of regenerated fiber Bragg grating sensors with long-term stability. Optics Express, 2016, 24, 21897.	3.4	26
202	Alloying of self-organized semiconductor 3D islands. Journal of Experimental Nanoscience, 2006, 1, 279-305.	2.4	25
203	Soft-landing electrospray ion beam deposition of sensitive oligoynes on surfaces in vacuum. International Journal of Mass Spectrometry, 2015, 377, 228-234.	1.5	25
204	Pentacene on Ni(111): room-temperature molecular packing and temperature-activated conversion to graphene. Nanoscale, 2015, 7, 3263-3269.	5.6	25
205	Green synthesis of near infrared core/shell quantum dots for photocatalytic hydrogen production. Nanotechnology, 2016, 27, 495405.	2.6	25
206	Photoelectrochemical properties of BiMnO 3 thin films and nanostructures. Journal of Power Sources, 2017, 365, 162-168.	7.8	25
207	1D/2D Cobaltâ€Based Nanohybrids as Electrocatalysts for Hydrogen Generation. Advanced Functional Materials, 2020, 30, 1908467.	14.9	25
208	Self-assembly of rubrene on Cu(111). Nanotechnology, 2008, 19, 424021.	2.6	24
209	2D Self-Assembly of Fused Oligothiophenes: Molecular Control of Morphology. ACS Nano, 2012, 6, 7973-7980.	14.6	24
210	Hollow micro/nanostructured materials prepared by ion exchange synthesis and their potential applications. New Journal of Chemistry, 2014, 38, 1883-1904.	2.8	24
211	Tailoring the Heterostructure of Colloidal Quantum Dots for Ratiometric Optical Nanothermometry. Small, 2020, 16, e2000804.	10.0	24
212	Playing Tetris at the nanoscale. Surface Science, 2006, 600, 1-5.	1.9	23
213	In situinvestigation of explosive crystallization in a-Ge: Experimental determination of the interface response function using dynamic transmission electron microscopy. Journal of Applied Physics, 2014, 116, 093512.	2.5	23
214	Room-temperature surface-assisted reactivity of a melanin precursor: silver metal–organic coordination <i>versus</i> covalent dimerization on gold. Nanoscale, 2018, 10, 16721-16729.	5.6	23
215	PLLA scaffolds with controlled architecture as potential microenvironment for in vitro tumor model. Tissue and Cell, 2019, 58, 33-41.	2.2	23
216	Ferroelectric polarization-enhanced charge separation in quantum dots sensitized semiconductor hybrid for photoelectrochemical hydrogen production. Nano Energy, 2021, 81, 105626.	16.0	23

#	Article	IF	CITATIONS
217	Semi-transparent luminescent solar concentrators based on plasmon-enhanced carbon dots. Journal of Materials Chemistry A, 2021, 9, 23345-23352.	10.3	23
218	High efficiency photoelectrochemical hydrogen generation using eco-friendly Cu doped Zn-In-Se colloidal quantum dots. Nano Energy, 2021, 88, 106220.	16.0	23
219	Inducing Nonlocal Reactions with a Local Probe. ACS Nano, 2009, 3, 3347-3351.	14.6	22
220	Highly Emissive and Electrochemically Stable Thienylene Vinylene Oligomers and Copolymers: An Unusual Effect of Alkylsulfanyl Substituents. Advanced Functional Materials, 2010, 20, 1661-1669.	14.9	22
221	Self-organization of an optomagnetic CoFe <sub>2</sub> O <sub>4</sub> –ZnS nanocomposite: preparation and characterization. Journal of Materials Chemistry C, 2015, 3, 3935-3945.	5.5	22
222	Nanofiber-supported CuS nanoplatelets as high efficiency counter electrodes for quantum dot-based photoelectrochemical hydrogen production. Materials Chemistry Frontiers, 2017, 1, 65-72.	5.9	22
223	Tailoring the interfacial structure of colloidal "giant―quantum dots for optoelectronic applications. Nanoscale, 2018, 10, 17189-17197.	5.6	22
224	CuS/Graphene Nanocomposite as a Transparent Conducting Oxide and Pt-Free Counter Electrode for Dye-Sensitized Solar Cells. Journal of the Electrochemical Society, 2019, 166, H3065-H3073.	2.9	22
225	High-Response, Ultrafast-Speed, and Self-Powered Photodetection Achieved in InP@ZnS-MoS <sub>2</sub> Phototransistors with Interdigitated Pt Electrodes. ACS Applied Materials & Interfaces, 2020, 12, 31382-31391.	8.0	22
226	Recovery of electro-mechanical properties inside self-healing composites through microencapsulation of carbon nanotubes. Scientific Reports, 2020, 10, 2973.	3.3	22
227	Self-assembly of indole-2-carboxylic acid at graphite and gold surfaces. Journal of Chemical Physics, 2015, 142, 101923.	3.0	21
228	Graphene oxide/cobalt-based nanohybrid electrodes for robust hydrogen generation. Applied Catalysis B: Environmental, 2019, 245, 167-176.	20.2	21
229	Water-dispersible polyaniline/graphene oxide counter electrodes for dye-sensitized solar cells: Influence of synthesis route on the device performance. Solar Energy, 2020, 207, 1202-1213.	6.1	21
230	Catalytic Hydrogen Evolution of NaBH4 Hydrolysis by Cobalt Nanoparticles Supported on Bagasse-Derived Porous Carbon. Nanomaterials, 2021, 11, 3259.	4.1	21
231	The influence of the gas environment on morphology and chemical composition of surfaces micro-machined with a femtosecond laser. Applied Surface Science, 2014, 320, 455-465.	6.1	20
232	Modulating Exciton Dynamics in Composite Nanocrystals for Excitonic Solar Cells. Journal of Physical Chemistry Letters, 2015, 6, 2489-2495.	4.6	20
233	Near-Infrared Colloidal Manganese-Doped Quantum Dots: Photoluminescence Mechanism and Temperature Response. ACS Photonics, 2019, 6, 2421-2431.	6.6	20
234	Enhanced Photocurrent Generation in Protonâ€Irradiated "Giant―CdSe/CdS Core/Shell Quantum Dots. Advanced Functional Materials, 2019, 29, 1904501.	14.9	20

#	Article	IF	CITATIONS
235	Hybrid surface passivation of PbS/CdS quantum dots for efficient photoelectrochemical hydrogen generation. Applied Surface Science, 2020, 530, 147252.	6.1	20
236	Gold nanoparticle decorated carbon nanotube nanocomposite for dye-sensitized solar cell performance and stability enhancement. Chemical Engineering Journal, 2021, 421, 127756.	12.7	20
237	Shape-stabilized phase change composites enabled by lightweight and bio-inspired interconnecting carbon aerogels for efficient energy storage and photo-thermal conversion. Journal of Materials Chemistry A, 2022, 10, 13556-13569.	10.3	20
238	Ensuring Homology between 2D and 3D Molecular Crystals. Langmuir, 2007, 23, 11980-11985.	3.5	19
239	Multiexponential photoluminescence decay of blinking nanocrystal ensembles. Physical Review B, 2009, 80, .	3.2	19
240	Reply to "Comment on â€~Insight into Organometallic Intermediate and Its Evolution to Covalent Bonding in Surface-Confined Ullmann Polymerization'― ACS Nano, 2014, 8, 1969-1971.	14.6	19
241	Structure versus properties in <i>α</i> -Fe <sub>2</sub> O <sub>3</sub> nanowires and nanoblades. Nanotechnology, 2016, 27, 035702.	2.6	19
242	Towards Longâ€Term Thermal Stability of Dye‧ensitized Solar Cells Using Multiwalled Carbon Nanotubes. ChemPlusChem, 2018, 83, 682-690.	2.8	18
243	Direct Measurement of Electronic Band Structure in Single Quantum Dots of Metal Chalcogenide Composites. Small, 2018, 14, e1801668.	10.0	18
244	Synthesis of highly efficient Cu2ZnSnSxSe4â^'x (CZTSSe) nanosheet electrocatalyst for dye-sensitized solar cells. Electrochimica Acta, 2020, 340, 135954.	5.2	18
245	Constructing quantum dots sensitized TiO2 nanotube p-n heterojunction for photoelectrochemical hydrogen generation. Chemical Engineering Journal, 2022, 446, 137312.	12.7	18
246	Nanostenciling of Functional Materials by Room Temperature Pulsed Laser Deposition. IEEE Nanotechnology Magazine, 2006, 5, 470-477.	2.0	17
247	Luminescent silicon nanostructures synthesized by laser ablation. Physica Status Solidi (A) Applications and Materials Science, 2007, 204, 1623-1638.	1.8	17
248	Towards ferroelectric and multiferroic nanostructures and their characterisation. International Journal of Nanotechnology, 2008, 5, 930.	0.2	17
249	Defect-induced enhanced photocatalytic activities of reduced <i>î±</i> -Fe <sub>2</sub> O <sub>3</sub> nanoblades. Nanotechnology, 2016, 27, 295703.	2.6	17
250	Controlled synthesis of near-infrared quantum dots for optoelectronic devices. Nanoscale, 2017, 9, 16843-16851.	5.6	17
251	Covalent organic frameworks from a monomer with reduced symmetry: polymorphism and Sierpiński triangles. Chemical Communications, 2019, 55, 13586-13589.	4.1	17
252	High performance BiFeO3 ferroelectric nanostructured photocathodes. Journal of Chemical Physics, 2020. 153. 084705.	3.0	17

#	Article	IF	CITATIONS
253	Role of Carbon Nanotubes to Enhance the Long-Term Stability of Dye-Sensitized Solar Cells. ACS Photonics, 2020, 7, 653-664.	6.6	17
254	Electrophoretic deposition of collagen/chitosan films with copper-doped phosphate glasses for orthopaedic implants. Journal of Colloid and Interface Science, 2022, 607, 869-880.	9.4	17
255	Seeing both sides. Nature Chemistry, 2010, 2, 344-345.	13.6	16
256	In situ coating of diatom frustules with silver nanoparticles. Green Chemistry, 2013, 15, 2060.	9.0	16
257	Efficient and stable hydrogen evolution based on earth-abundant SnSe nanocrystals. Applied Catalysis B: Environmental, 2020, 264, 118526.	20.2	16
258	Two-dimensional functionalized hexagonal boron nitride for quantum dot photoelectrochemical hydrogen generation. Journal of Materials Chemistry A, 2020, 8, 20698-20713.	10.3	16
259	Preferred Film Orientation to Achieve Stable and Efficient Sn–Pb Binary Perovskite Solar Cells. ACS Applied Materials & Interfaces, 2021, 13, 10822-10836.	8.0	16
260	Multielement synergetic effect of NiFe <sub>2</sub> O <sub>4</sub> and h-BN for improving the dehydrogenation properties of LiAlH <sub>4</sub> . Inorganic Chemistry Frontiers, 2021, 8, 3111-3126.	6.0	16
261	Packing-induced electronic structure changes in bundled single-wall carbon nanotubes. Applied Physics Letters, 2005, 87, 103106.	3.3	15
262	Fullerene on Nitrogen-Adsorbed Cu(001) Nanopatterned Surfaces: From Preferential Nucleation to Layer-by-Layer Growth. Journal of Physical Chemistry C, 2008, 112, 10187-10192.	3.1	15
263	Nanoscale patterning of functional perovskite-type complex oxides by pulsed laser deposition through a nanostencil. Applied Surface Science, 2010, 256, 4777-4783.	6.1	15
264	Expanding the Scope of Molecular Self-organization Studies through Temperature Control at the Solution/Solid Interface. Australian Journal of Chemistry, 2011, 64, 1299.	0.9	15
265	Graphene nanoribbon-TiO2-quantum dots hybrid photoanode to boost the performance of photoelectrochemical for hydrogen generation. Catalysis Today, 2020, 340, 161-169.	4.4	15
266	Effect of pressure on the properties of a NASICON Li <sub>1.3</sub> Al <sub>0.3</sub> Ti <sub>1.7</sub> (PO <sub>4</sub> ) <sub>3</sub> nanofiber solid electrolyte. Journal of Materials Chemistry A, 2021, 9, 13688-13696.	10.3	15
267	Site-controlled growth of Ge nanostructures on Si(100) via pulsed laser deposition nanostenciling. Applied Physics Letters, 2007, 91, 113112.	3.3	14
268	EFFECT OF EPITAXIAL STRAIN ON THE STRUCTURAL AND FERROELECTRIC PROPERTIES OF <font>Bi</font> <sub>2</sub> <font>FeCrO</font> <sub>6</sub> THIN FILMS. Functional Materials Letters, 2010, 03, 83-88.	1.2	14
269	Selfâ€Assembly of a Halogenated Molecule on Oxideâ€Passivated Cu(110). Chemistry - an Asian Journal, 2013, 8, 1813-1817.	3.3	14
270	Tip-induced C–H activation and oligomerization of thienoanthracenes. Chemical Communications, 2014, 50, 8791-8793.	4.1	14

#	Article	IF	CITATIONS
271	Electrical and Optical Properties of Transparent Conducting <i>p</i> â€Type SrTiO <sub>3</sub> Thin Films. Journal of the American Ceramic Society, 2016, 99, 226-233.	3.8	14
272	Dual emission and optical gain in PbS/CdS nanocrystals: Role of shell volume and of core/shell interface. Physical Review B, 2017, 96, .	3.2	14
273	Ultra-small colloidal heavy-metal-free nanoplatelets for efficient hydrogen generation. Applied Catalysis B: Environmental, 2019, 250, 234-241.	20.2	14
274	MoS2-supported on free-standing TiO2-nanotubes for efficient hydrogen evolution reaction. International Journal of Hydrogen Energy, 2020, 45, 4468-4480.	7.1	14
275	Modulating the 0D/2D Interface of Hybrid Semiconductors for Enhanced Photoelectrochemical Performances. Small Methods, 2021, 5, e2100109.	8.6	14
276	Role of surface engineering of hybrid structure for high performance quantum dots based photoelectrochemical hydrogen generation. Chemical Engineering Journal, 2022, 429, 132425.	12.7	14
277	The Self-Healing Capability of Carbon Fibre Composite Structures Subjected to Hypervelocity Impacts Simulating Orbital Space Debris. ISRN Nanomaterials, 2012, 2012, 1-16.	0.7	14
278	Atomic Identification of Interfaces in Individual Core@shell Quantum Dots. Advanced Science, 2021, 8, e2102784.	11.2	14
279	Role of Interfacial Engineering of "Giant―Core–Shell Quantum Dots. ACS Applied Energy Materials, 2022, 5, 1447-1459.	5.1	14
280	Materials Science in the Developing World: Challenges and Perspectives for Africa. Advanced Materials, 2008, 20, 4627-4640.	21.0	13
281	Controlling anatase coating of diatom frustules by varying the binding layer. CrystEngComm, 2012, 14, 3446.	2.6	13
282	Ruthenium Grubbs' catalyst nanostructures grown by UV-excimer-laser ablation for self-healing applications. Applied Surface Science, 2012, 258, 9800-9804.	6.1	13
283	One-pot synthesis of theranostic nanocapsules with lanthanide doped nanoparticles. Chemical Science, 2020, 11, 6653-6661.	7.4	13
284	Coordinating light management and advance metal nitride interlayer enables MAPbI3 solar cells with >21.8% efficiency. Nano Energy, 2022, 92, 106765.	16.0	13
285	Semiconductor and insulator nanostructures: challenges and opportunities. Microelectronic Engineering, 2005, 80, 448-456.	2.4	12
286	High-frequency electromagnetic properties of epitaxial Bi2FeCrO6 thin films grown by pulsed laser deposition. Applied Physics Letters, 2011, 99, 183505.	3.3	12
287	Ferroelectric switching in Bi <sub>4</sub> Ti <sub>3</sub> O <sub>12</sub> nanorods. IEEE Transactions on Ultrasonics, Ferroelectrics, and Frequency Control, 2012, 59, 1903-1911.	3.0	12
288	Superparamagnetic imposed diatom frustules for the effective removal of phosphates. Green Chemistry, 2014, 16, 82-85.	9.0	12

#	Article	IF	CITATIONS
289	With great structure comes great functionality: Understanding and emulating spider silk. Journal of Materials Research, 2015, 30, 108-120.	2.6	12
290	Tailoring the Reaction Path in the On-Surface Chemistry of Thienoacenes. Journal of Physical Chemistry C, 2015, 119, 22432-22438.	3.1	12
291	Silk fibroin-derived polypeptides additives to promote hydroxyapatite nucleation in dense collagen hydrogels. PLoS ONE, 2019, 14, e0219429.	2.5	12
292	On‣urface Decarboxylation Coupling Facilitated by Lockâ€ŧoâ€Unlock Variation of Molecules upon the Reaction. Angewandte Chemie - International Edition, 2021, 60, 17435-17439.	13.8	12
293	A Flexible Electrochemical Biosensor Based on NdNiO <sub>3</sub> Nanotubes for Ascorbic Acid Detection. ACS Applied Nano Materials, 2022, 5, 3394-3405.	5.0	12
294	Binding Geometry of Hydrogen-Bonded Chain Motif in Self-Assembled Gratings and Layers on Ag(111). Langmuir, 2012, 28, 14291-14300.	3.5	11
295	Multiferroic nanoscale Bi2FeCrO6 material for spintronic-related applications. Nanoscale, 2012, 4, 5588.	5.6	11
296	Influence of silicon dangling bonds on germanium thermal diffusion within SiO2 glass. Applied Physics Letters, 2014, 104, .	3.3	11
297	Template-Driven Dense Packing of Pentagonal Molecules in Monolayer Films. Nano Letters, 2018, 18, 7570-7575.	9.1	11
298	A modified â€~skeleton/skin' strategy for designing CoNiP nanosheets arrayed on graphene foam for on/off switching of NaBH <sub>4</sub> hydrolysis. RSC Advances, 2020, 10, 26834-26842.	3.6	11
299	Encapsulation of Dual Emitting Giant Quantum Dots in Silica Nanoparticles for Optical Ratiometric Temperature Nanosensors. Applied Sciences (Switzerland), 2020, 10, 2767.	2.5	11
300	Mo-doped ZnV2O6/reduced graphene oxide photoanodes for solar hydrogen production. Electrochimica Acta, 2021, 382, 138333.	5.2	11
301	Highly stable air processed perovskite solar cells by interfacial layer engineering. Chemical Engineering Journal, 2021, 423, 130334.	12.7	11
302	Temperature-Dependence Photoelectrochemical Hydrogen Generation Based on Alloyed Quantum Dots. Journal of Physical Chemistry C, 2022, 126, 174-182.	3.1	11
303	Structural effect of Low-dimensional carbon nanostructures on Long-term stability of dye sensitized solar cells. Chemical Engineering Journal, 2022, 435, 135037.	12.7	11
304	Enhanced Hydrogen Storage Properties of LiAlH <sub>4</sub> by Excellent Catalytic Activity of XTiO <sub>3</sub> @ <i>h</i> â€BN (X = Co, Ni). Advanced Functional Materials, 2022, 32, .	14.9	11
305	Heterostructured core/gradient multi-shell quantum dots for high-performance and durable photoelectrochemical hydrogen generation. Nano Energy, 2022, 100, 107524.	16.0	11
306	Nanofiber-Structured TiO2Nanocrystals as a Scattering Layer in Dye-Sensitized Solar Cells. ECS Journal of Solid State Science and Technology, 2017, 6, N32-N37.	1.8	10

#	Article	IF	CITATIONS
307	Cure kinetics of poly (5-ethylidene-2-norbornene) with 2nd generation Hoveyda-Grubbs' catalyst for self-healing applications. Polymer, 2018, 153, 1-8.	3.8	10
308	Bidirectional Superionic Conduction in Surface-Engineered 2D Hexagonal Boron Nitrides. ACS Applied Materials & Interfaces, 2021, 13, 6532-6544.	8.0	10
309	Unlocking the effects of Cu doping in heavy-metal-free AgIn <sub>5</sub> S <sub>8</sub> quantum dots for highly efficient photoelectrochemical solar energy conversion. Journal of Materials Chemistry C, 2021, 9, 9610-9618.	5.5	10
310	A graphene-like nanoribbon for efficient bifunctional electrocatalysts. Journal of Materials Chemistry A, 2021, 9, 26688-26697.	10.3	10
311	Ambipolar operation of hybrid SiC-carbon nanotube based thin film transistors for logic circuits applications. Applied Physics Letters, 2012, 101, 043121.	3.3	9
312	Temperature-induced molecular reorganization on Au(111) driven by oligomeric defects. Nanoscale, 2019, 11, 19468-19476.	5.6	9
313	Self-assembly of 5,6-dihydroxyindole-2-carboxylic acid: polymorphism of a eumelanin building block on Au(111). Nanoscale, 2019, 11, 5422-5428.	5.6	9
314	Low-Cost, Air-Processed Quantum Dot Solar Cells via Diffusion-Controlled Synthesis. ACS Applied Materials & Interfaces, 2020, 12, 36301-36310.	8.0	9
315	BiVO4 ceramics for high-sensitivity and high-temperature optical thermometry. Journal of Luminescence, 2021, 230, 117739.	3.1	9
316	Identification of Topotactic Surface onfined Ullmannâ€Polymerization. Small, 2021, 17, e2103044.	10.0	9
317	Nanoelectromagnetic of the N-doped single wall carbon nanotube in the extremely high frequency band. Nanoscale, 2017, 9, 14192-14200.	5.6	8
318	Planar Anchoring of C <sub>70</sub> Liquid Crystals Using a Covalent Organic Framework Template. Small, 2019, 15, e1903294.	10.0	8
319	Two-dimensional polymers grow up. Science, 2019, 366, 1308-1309.	12.6	8
320	Solution-Processed p-Type Copper Thiocyanate (CuSCN) Enhanced Sensitivity of PbS-Quantum-Dots-Based Photodiode. ACS Photonics, 2020, 7, 1628-1635.	6.6	8
321	Electron transfer in a semiconductor heterostructure interface through electrophoretic deposition and a linker-assisted method. CrystEngComm, 2020, 22, 1664-1673.	2.6	8
322	Allâ€Ambientâ€Processed CuSCN as an Inexpensive Alternative to Spiroâ€OMeTAD for Perovskiteâ€Based Devices. Energy Technology, 2021, 9, .	3.8	8
323	Oxygen-promoted synthesis of armchair graphene nanoribbons on Cu(111). Science China Chemistry, 2021, 64, 636-641.	8.2	8
324	A low-loss origami plasmonic waveguide. Science, 2017, 357, 452-453.	12.6	7

#	Article	IF	CITATIONS
325	An â€~ice-melting' kinetic control strategy for highly photocatalytic organic nanocrystals. Journal of Materials Chemistry A, 2020, 8, 25275-25282.	10.3	7
326	Hybrid PCDTBT:PCBM:Graphene-Nanoplatelet Photoabsorbers. Journal of the Electrochemical Society, 2020, 167, 136504.	2.9	7
327	Transformations of Molecular Frameworks by Host–Guest Response: Novel Routes toward Two-Dimensional Self-Assembly at the Solid–Liquid Interface. Japanese Journal of Applied Physics, 2011, 50, 08LA02.	1.5	7
328	Tandem Desulfurization/C–C Coupling Reaction of Tetrathienylbenzenes on Cu(111): Synthesis of Pentacene and an Exotic Ladder Polymer. ACS Nano, 2022, 16, 6506-6514.	14.6	7
329	Brewery spent grain derived carbon dots for metal sensing. RSC Advances, 2022, 12, 11621-11627.	3.6	7
330	Alternative Uses of Luminescent Solar Concentrators. Nanoenergy Advances, 2022, 2, 222-240.	7.7	7
331	High-performance thin-film-transistors based on semiconducting-enriched single-walled carbon nanotubes processed by electrical-breakdown strategy. Applied Surface Science, 2015, 328, 349-355.	6.1	6
332	Asymmetry in supramolecular assembly. Science, 2016, 353, 1098-1099.	12.6	6
333	2D Supramolecular networks of dibenzonitrilediacetylene on Ag(111) stabilized by intermolecular hydrogen bonding. Physical Chemistry Chemical Physics, 2017, 19, 10602-10610.	2.8	6
334	Epitaxial patterned Bi <sub>2</sub> FeCrO <sub>6</sub> nanoisland arrays with room temperature multiferroic properties. Nanoscale Advances, 2019, 1, 2139-2145.	4.6	6
335	Oxygenâ€Induced 1D to 2D Transformation of Onâ€Surface Organometallic Structures. Small, 2020, 16, 2002393.	10.0	6
336	Synthesis of Electrospun NASICON Li <sub>1.5</sub> Al <sub>0.5</sub> Ge <sub>1.5</sub> (PO <sub>4</sub> ) <sub>3</sub> Solid Electrolyte Nanofibers by Control of Germanium Hydrolysis. Journal of the Electrochemical Society, 2021, 168, 110512.	2.9	6
337	Onâ€Surface Synthesis of Unsaturated Hydrocarbon Chains through Câ^'S Activation. Chemistry - A European Journal, 2022, 28, .	3.3	6
338	Unzipping oyster shell. RSC Advances, 2013, 3, 3284.	3.6	5
339	Surface structure of Pd(111) with less than half a monolayer of Zn. Physical Chemistry Chemical Physics, 2013, 15, 12488.	2.8	5
340	Characterization of individual multifunctional nanoobjects with restricted geometry. Phase Transitions, 2013, 86, 635-650.	1.3	5
341	Photoluminescence mapping of oxygen-defect emission for nanoscale spatial characterization of fiber Bragg gratings. Journal of Applied Physics, 2014, 116, 064906.	2.5	5
342	Thermal evolution of the submonolayer near-surface alloy of ZnPd on Pd(111). Physical Chemistry Chemical Physics, 2014, 16, 4764.	2.8	5

#	Article	IF	CITATIONS
343	Stable multilevel memories. Nature Photonics, 2016, 10, 434-436.	31.4	5
344	Blocking germanium diffusion inside silicon dioxide using a co-implanted silicon barrier. Journal of Applied Physics, 2018, 123, .	2.5	5
345	Failure analysis of self-healing epoxy resins using microencapsulated 5E2N and carbon nanotubes. Smart Materials and Structures, 2021, 30, 025011.	3.5	5
346	In situnanoscale mapping of the chemical composition of surfaces and 3D nanostructures by photoelectron spectromicroscopy. Nanotechnology, 2008, 19, 265703.	2.6	4
347	Mechanical and electrical properties of epitaxial Si nanowires grown by pulsed laser deposition. Journal of Physics Condensed Matter, 2012, 24, 445008.	1.8	4
348	Blending organic building blocks. Nature Photonics, 2012, 6, 639-640.	31.4	4
349	Rising from the Falls. Nature Materials, 2012, 11, 187-188.	27.5	4
350	Enhanced stability of higher UV-densified Fiber Bragg Gratings after thermal regeneration. Optics Communications, 2019, 435, 345-349.	2.1	4
351	Inhibition of nucleation and crystal growth of calcium carbonate in hard waters using Paronychia arabica in an arid desert region. Water and Environment Journal, 2020, 34, 979-987.	2.2	4
352	Influence of Ti <sup>IV</sup> substitution on the properties of a Li <sub>1.5</sub> Al <sub>0.5</sub> Ge <sub>1.5</sub> (PO <sub>4</sub> ) <sub>3</sub> nanofiber-based solid electrolyte. Nanoscale, 2022, 14, 5094-5101.	5.6	4
353	Design of MOFâ€Derived NiOâ€Carbon Nanohybrids Photocathodes Sensitized with Quantum Dots for Solar Hydrogen Production. Small, 2022, 18, e2201815.	10.0	4
354	Memory operation devices based on light-illumination ambipolar carbon-nanotube thin-film-transistors. Journal of Applied Physics, 2015, 118, .	2.5	3
355	Reaction pathways for pyridine adsorption on silicon (0 0 1). Journal of Physics Condensed Matter, 2015, 27, 054001.	1.8	3
356	Dual Template Engaged Synthesis of Hollow Ballâ€inâ€Tube Asymmetrical Structured Ceria. Particle and Particle Systems Characterization, 2018, 35, 1700367.	2.3	3
357	Direct on-surface synthesis of gold–phthalocyanine <i>via</i> cyclization of cyano-groups with gold adatoms. Materials Chemistry Frontiers, 2019, 3, 1406-1410.	5.9	3
358	Epitaxial growth and defect repair of heterostructured CuInSe <sub>x</sub> S <sub>2â^'x</sub> /CdSeS/CdS quantum dots. Nanoscale, 2019, 11, 19529-19535.	5.6	3
359	Rational synthesis of novel "giant―CuInTeSe/CdS core/shell quantum dots for optoelectronics. Nanoscale, 2021, 13, 15301-15310.	5.6	3
360	Probing the Thermodynamics of Moiré Patterns in Molecular Self-Assembly at the Liquid–Solid Interface. Chemistry of Materials, 2022, 34, 2449-2457.	6.7	3

#	Article	IF	CITATIONS
361	Co-mediated nucleation of erbium/silicon nanoclusters in fused silica. Journal of Materials Research, 2015, 30, 3003-3010.	2.6	2
362	Influence of photo-luminescent CdSe/CdS core shell quantum dots in solar cell efficiency. Journal of Physics: Conference Series, 2016, 773, 012088.	0.4	2
363	Benzene and Pyridine on Silicon (001): A Trial Ground for Long-Range Corrections in Density Functional Theory. Journal of Physical Chemistry C, 2017, 121, 10484-10500.	3.1	2
364	Quantum Dots: Quantum Dotsâ€Based Photoelectrochemical Hydrogen Evolution from Water Splitting (Adv. Energy Mater. 12/2021). Advanced Energy Materials, 2021, 11, 2170047.	19.5	2
365	On‣urface Decarboxylation Coupling Facilitated by Lockâ€ŧoâ€Unlock Variation of Molecules upon the Reaction. Angewandte Chemie, 2021, 133, 17575-17579.	2.0	2
366	Luminescent Solar Concentrators: Near Infrared, Highly Efficient Luminescent Solar Concentrators (Adv. Energy Mater. 11/2016). Advanced Energy Materials, 2016, 6, .	19.5	1
367	Solar Concentrators: Absorption Enhancement in "Giant―Core/Alloyed-Shell Quantum Dots for Luminescent Solar Concentrator (Small 38/2016). Small, 2016, 12, 5368-5368.	10.0	1
368	Enhanced radiation resistance of near-infrared photoluminescence emission induced by Er/Si nanoclustering. Materials and Design, 2017, 126, 57-63.	7.0	1
369	Nature and Chinese Art Inspire Materials for Light Harvesting. Matter, 2020, 3, 24-26.	10.0	1
370	Bidirectional Phase Transformation of Supramolecular Networks Using Two Molecular Signals. ACS Nano, 2022, 16, 1560-1566.	14.6	1
371	Photovoltaic properties of hybrid c-Si/ZnO nanorods solar cells. Materials Advances, 0, , .	5.4	1
372	Temperature Sensors: Ultrasensitive, Biocompatible, Self-Calibrating, Multiparametric Temperature Sensors (Small 43/2015). Small, 2015, 11, 5740-5740.	10.0	0
373	Quantum Dots: Nearâ€Infrared Colloidal Quantum Dots for Efficient and Durable Photoelectrochemical Solarâ€Driven Hydrogen Production (Adv. Sci. 3/2016). Advanced Science, 2016, 3, .	11.2	0
374	Probing properties of molecule-based interface systems: general discussion and Discussion of the Concluding Remarks. Faraday Discussions, 2017, 204, 503-530.	3.2	0
375	A bridge for charge carriers. Nature Energy, 2019, 4, 910-911.	39.5	0
376	Four-fold multifunctional properties in self-organized layered ferrite. Ceramics International, 2020, 46, 28621-28630.	4.8	0
377	Supporting the Development and Deployment of Sustainable Energy Technologies Through Targeted Scientific Training. , 2015, , 231-233.		0

Temperature-dependent Raman spectroscopy studies of fibers. , 2016, , .

#	Article	IF	CITATIONS
379	Multifunctional Materials For Emerging Solar Technologies. , 2018, , .		Ο